PRT-6 | 775

ASAT

MILITARY TECHNICAL COLLEGE
CAIRO - EGYPT

FURTHER PROBLEMS AFFECTING THE PRODUCTION OF ELLIPTICAL HOLES BY ECM

M. S. HEWIDY *

ABSTRACT

ECM has found wide applications in aerospace industries. However, tool design in ECM is still a problem which delays the use of this process. This paper has focused attention on some of the problems that are to be studied before it would be possible to obtain an analytical design of toolings for ECM.

Furthermore, this paper has emphasized that each component in ECM presents its own particular problems and each must be treated on its own merits as has been shown through producing the elliptical hole shape.

Inequality of electrolyte distribution, different electrolyte path lengths and variations in current density have been found to be the main features that characterize the nature of the elliptical hole shape by ECM. Resistance model technique has been suggested and modified to use for analysis of the elliptical hole shape. A parametric study of the process which highlights certain guidelines for ECM tooling designer is also presented.

Experimental results have revealed significant variations in the resultant side gap length at major and minor diameters of the tool. The experimental tests have been in agreement with the present analysis. Further, resistance model technique has proved its validity for use in evaluating the power consumption in ECM.

INTRODUCTION

Electrochemical machining (ECM), defined as the controlled anodic corrosion process, is commonly employed to shape components made of difficult-to machine metals required by such sophisticated industries as aerospace and gas turbine industries. The last two decades have witnessed rapid advances in the field of ECM, and it is expected that

---

* Assistant Professor, Production Engineering & Machine Design Department, Faculty of Engineering & Technology, Menoufia University, Shebin El-Kom, Egypt.

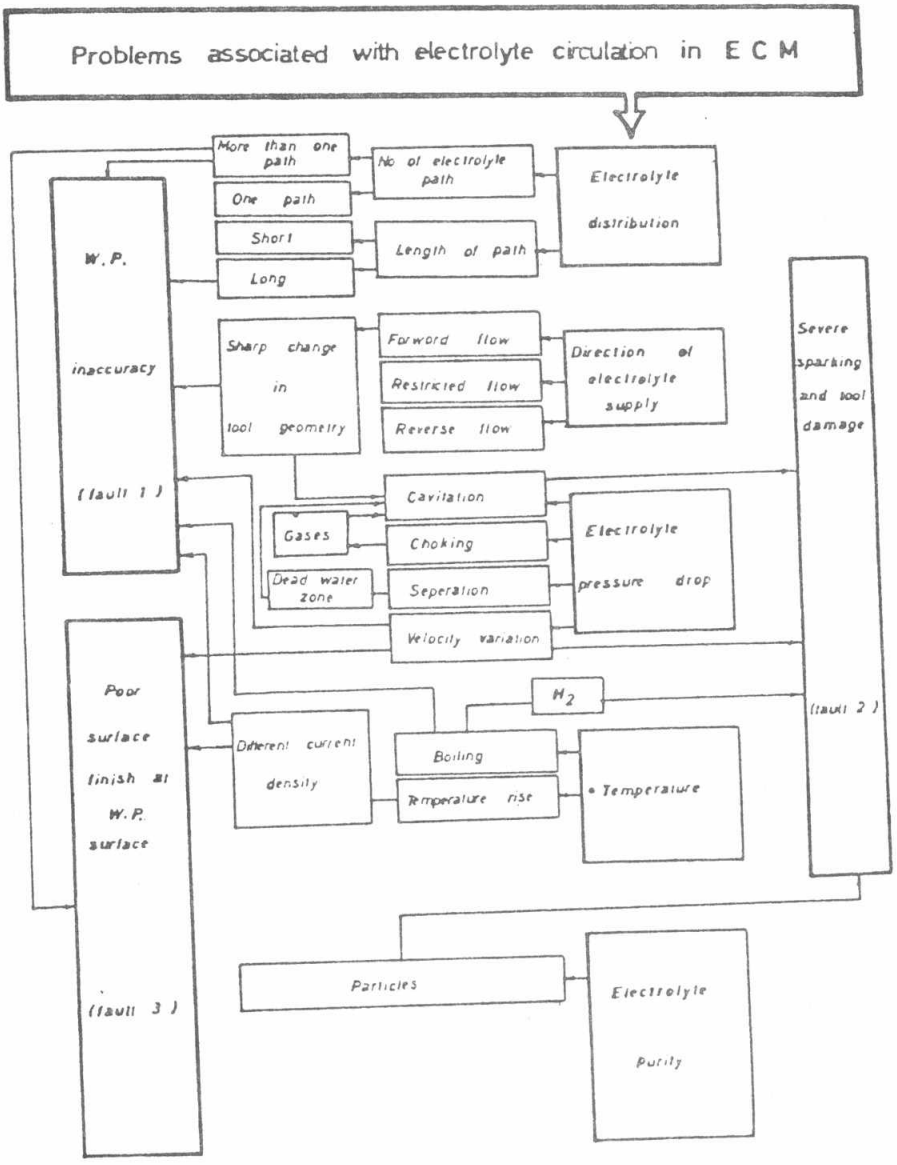

Fig.1. Proposed simplified scheme for the electrolyte problems in E C M

in the few years to come, this process would find ready applications in a wide variety of production industries.

It is, however, felt that the capabilities of this process have not been fully exploited, due to the difficulties encountered in the design of toolings for the given workpiece. The biggest problem facing the tool designer in ECM is how to achieve a strict control on electrolyte temperature and pressure stability in all the interelectrode gap. Correct electrode flow across a tool is essential for its success and is the most important feature of the tool design. So, each component should be considered for full use of its natural features to achieve suitable flow.

A hole sinking operation in the ECM has been studied, using tools of different shapes : Ebeid [1] summarized some published papers about the problems the circular hole shaped encountered. Rectangular hole [2] and hexagonal hole [3] have also been studied to assess an empirical and theoretical relationship between tool dimensions and resultant workpiece profile

Elliptical holes by ECM have a complexity nature because of the non-uniform distribution of the electrolyte along the major and minor axes of the tool surface. The author has summarized, in Fig. 1, the main problems which may associate electrolyte circulation in ECM. Elliptical hole shaped constitutes the bulk of these problems, as the experimental investigations have revealed.

This paper has adopted the resistance model technique [2] to be valid enough to estimate the geometry of workpiece profile in ECM. The analytical technique in this work has been supported by some realistic and practical factors recognized in the present tests.

This paper also presents experimental verifications of the theory presented herein to emphasise its validity for use in the ECM process.

THEORETICAL ANALYSIS

For an accurate modelling of the cavity sinking process, all the electrolyte resistances in the interelectrode gap should be calculated accurately [4], as shown in Fig. 2. This technique has been successfully applied to several cases [2-4], and has proved to be valid.

Figure 2 shows that side gap in the direction of minor diameter ($Y_{\bar{b}}$) behaves in a similar way as the overcut length in case of circular holes. Thus,

$$Y_{\bar{b}} = \sqrt{v^2 Y_e^2 + 2 Y_e t}$$

where (Y_e) is the equilibrium gap in the frontal direction ($\bar{f}$) and can be calculated as follows :

$$Y_e = \frac{(v - \Delta v)\, k\, \epsilon}{f\, F\, \rho_w}$$

In the present work, experimental investigations have detected significant

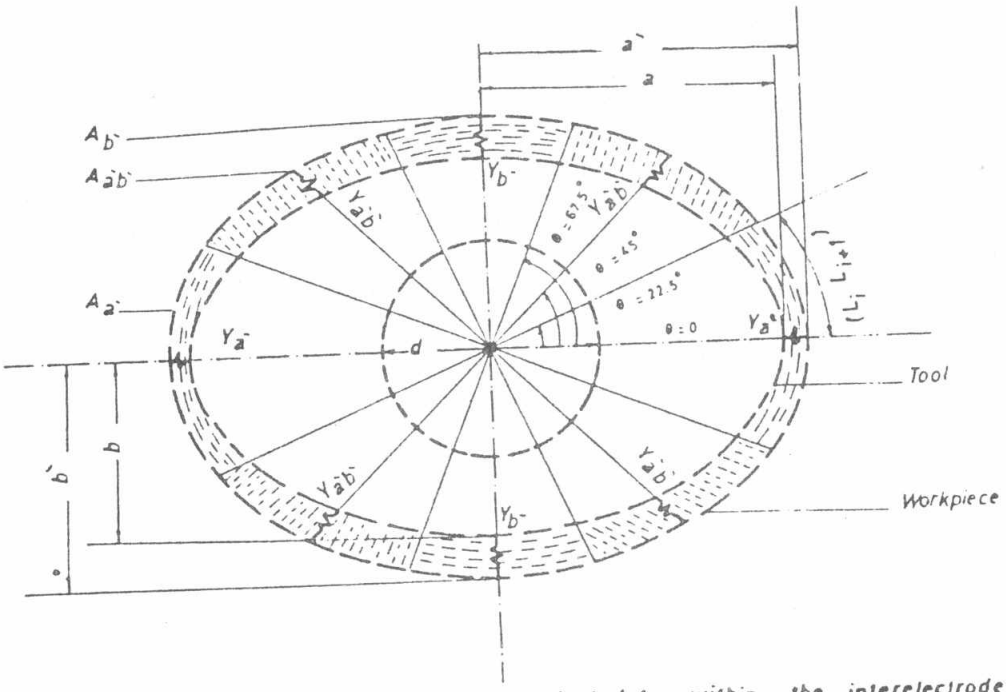

Fig. 2. Equivalent resistance of the electrolyte within the interelectrode gap for a hole operation using elliptical tool.

variations between side gaps at major and minor diameters of the elliptical tool. The relation between the two side gaps can be expressed as follows :

$$Y_{\bar{a}} = \lambda Y_{\bar{b}}$$

The side gap at the direction of the ellipse diameter ($Y_{\bar{a}\bar{b}}$) can be deduced from the general equation of the ellipse [5].

$$\frac{x^2}{\bar{a}^2} + \frac{Y^2}{\bar{b}^2} = 1 \qquad (4)$$

$$x = \frac{\bar{a}\,\bar{b}}{\sqrt{\bar{b}^2 + \bar{a}^2}} \qquad (5)$$

So, the diameter of the ellipse becomes

$$ou = \frac{\bar{a}\,\bar{b}\sqrt{2}}{\sqrt{\bar{b}^2 + \bar{a}^2}} \qquad (6)$$

The side gap length ($Y_{\bar{a}\,\bar{b}}$) is equal to

$$Y_{\bar{a}\,\bar{b}} = \frac{1}{2}\left[\frac{\bar{a}\,\bar{b}\sqrt{2}}{\sqrt{\bar{b}^2 + \bar{a}^2}} - \frac{a\,b\sqrt{2}}{\sqrt{b^2 + a^2}}\right] \qquad (7)$$

Experimental tests will reveal the accurate value of side gap correcting factor (λ). Then the workpiece profile can be constructed by knowing the two ellipse diameters.

$$\bar{a} = a + \lambda\,\bar{a} \qquad (4)$$

$$\bar{b} = b + \sqrt{\nu^2 Y_e^2 + 2 Y_e t} \qquad (5)$$

where a and b are the radii of the elliptical tool at major and minor axes respectively.

The variation in length of side gaps has been attributed to the inequality of electrolyte path length w.r.t. the surface of hole electrolyte supply.

For a whole sinking operation, using elliptical tool (Fig. 2), the equivalent resistance of the lectrolyte within the working gap can be derived as follows :

$$\frac{1}{R_{tot}} = \sum \frac{1}{R_{\bar{a}}} + \sum \frac{1}{R_{\bar{b}}} + \sum \frac{1}{R_{\bar{a}\,\bar{b}}} + \frac{1}{R_{\bar{f}}} \qquad (8)$$

The individual resistance in equation (8) is given by the general relationship :

$$R_i = \frac{Y_i}{K_i\,A_i} \qquad (9)$$

For a small element, it is assumed that:

$$K_{\bar{a}} = K_{\bar{b}} = K_{\bar{a}\,\bar{b}} = K_{\bar{f}} \tag{10}$$

Then

$$\frac{1}{R_{tot}} = \frac{2\,R_{\bar{b}}\,R_{\bar{a}\bar{b}}\,R_{\bar{f}} + 2\,R_{\bar{a}}\,R_{\bar{b}}\,R_{\bar{f}} + 4\,R_{\bar{a}}\,R_{\bar{b}}\,R_{\bar{f}} + R_{\bar{a}}\,R_{\bar{b}}\,R_{\bar{a}\bar{b}}}{R_{\bar{a}}\,R_{\bar{b}}\,R_{\bar{a}\bar{b}}\,R_{\bar{f}}} \tag{11}$$

The equivalent resistance becomes

$$R_{tot} = \frac{1}{K}\left[\frac{Y_{\bar{a}}\,Y_{\bar{b}}\,Y_{\bar{a}\bar{b}}\,Y_e \cdot A_{\bar{a}}^2\,A_{\bar{b}}^2\,A_{\bar{a}\bar{b}}^2\,A_{\bar{f}}^2}{2\,Y_{\bar{b}}\,Y_{\bar{a}\bar{b}}\,Y_e + 2Y_{\bar{a}}\,Y_{\bar{a}\bar{b}}\,Y_{\bar{f}} + 4\,Y_{\bar{a}}\,Y_{\bar{b}}\,Y_{\bar{f}} + Y_{\bar{a}}\,Y_{\bar{b}}\,Y_{\bar{a}\bar{b}}}\right] \tag{12}$$

The different side areas ($A_{\bar{a}}$, $A_{\bar{b}}$, and $A_{\bar{a}\,\bar{b}}$) of the workpiece profile can be computed through the determination of the corresponding arcs for these areas (Fig. 2).

The length of the arc of the elliptical curve is expressed by the formula of the ellipse in parametric form :

$$d\,(L_i\,L_{i+1}) = \int_{\theta_i}^{i+1} \sqrt{\left(\frac{dx}{d\theta}\right)^2 + \left(\frac{dy}{d\theta}\right)^2}\; d\theta \tag{13}$$

where $x = \bar{a}\,\sin\theta$ and $y = \bar{b}\,\cos\theta$ (14)

$$d\,(L_i\,L_{1+1}) = \int_{\theta_i}^{i+1} \sqrt{\bar{a}^2\,\cos^2\theta + \bar{b}^2\,\sin^2\theta}\; d\theta \tag{15}$$

Inserting the relation of ellipse eccentricity in equation (15), the general equation of length of elliptical curve can be obtained by the following equation

$$d(L_i\;L_{i+1}) = \bar{a}\int_{\theta_i}^{i+1}\left[1 - \frac{1}{2}e^2\sin^2\theta\,\frac{1}{8}e^4\sin\theta + \ldots\right] d\theta \tag{16}$$

$$= \theta + \frac{1}{4}e^2\cos\theta\sin\theta - \frac{1}{2}e^2 + \frac{1}{32}e^4\cos\theta\sin^3\theta$$

$$+ \frac{3}{64}e^4\cos\theta\sin\theta - \frac{3}{64}e^4\Big|_{\theta_i}^{i+1} \tag{17}$$

So,

$$d\,(L_i\,L_{i+1}) = \bar{a}\,(X)\Big|_{\theta_i}^{i+1} \tag{18}$$

The areas of workpiece profile ($A_{\bar{a}}$, $A_{\bar{b}}$ and $A_{\bar{a}\,\bar{b}}$) can be obtained as follows :

$$A_{\bar{a}} = 2\,\bar{a}\,(t + Y_e)\,(X)\Big|_{0^\circ}^{22.5^\circ} \tag{19}$$

$$A_{\bar{b}} = 2\,\bar{a}\,(t + Y_e)\,(X) \Big|_{67.5^\circ}^{90^\circ} \qquad (20)$$

$$A_{\bar{a}\,\bar{b}} = \bar{a}\,(t + Y_e)\,(X) \Big|_{22.2^\circ}^{67.5^\circ} \qquad (21)$$

$$A_{\bar{f}} = \pi\,(\bar{a}\,\bar{b}) \qquad (22)$$

Substituting equations 19, 20, and 22 in equation 12, the equivalent resistance of the interelectrode gap can be got.

The consumed current (I) can be obtained by the next equation :

$$I = \frac{(v - \Delta v)}{R_{tot}} \qquad (23)$$

The current density over the workpiece can be expressed as follows :

$$J = \frac{I}{A_{Frontal} + A_{Side}} \qquad (24)$$

$$= \frac{I}{\bar{a}\,\bar{b} + \pi\,(\bar{a} + \bar{b})\,(t + Y_e)} \qquad (25)$$

EXPEIMENTAL WORK

The general lay-out of the ECM equipment used in this investigation is shown in Fig. 2. Brass was used as a tool meterial. To guarantee smooth flow electrolyte, the tools were provided with rounded corners of about 0.5 to 1 mm radius. All workpieces (st. 37), have a thickness of about 15 mm. Workpiece fixture was connected to the machining cell through a press fit to get a better alignment as shown in Fig. 4.

To overcome the problem of temperature rise during the ECM processes, a large quantity of electrolyte was pumped through the working gap to minimize the temperature rise. Furthermore, the temperature was kept almost constant within 2 C through an adjustable thermostat connected to the control panel of the EC equipment. The resulting workpiece profiles were measured by the use of a projector with a magnification of 10 : 1.

RESULTS AND DISCUSSION

The present investigations have been carried out to optimize the working conditions in ECM, to get the elliptical hole shaped. Experimental tests have revealed variations in the side gap length at major and minor diameters of the elliptical tool. Figure 5 shows a comparison between tool geometry and resultant workpiece profile at various equilibrium gaps. All dismensions in Fig. 5 have been referred to the whole surface of the electrolyte supply. Figure 6 shows the plotting of the workpiece side gaps at major and minor diameters at different equilibrium gaps.

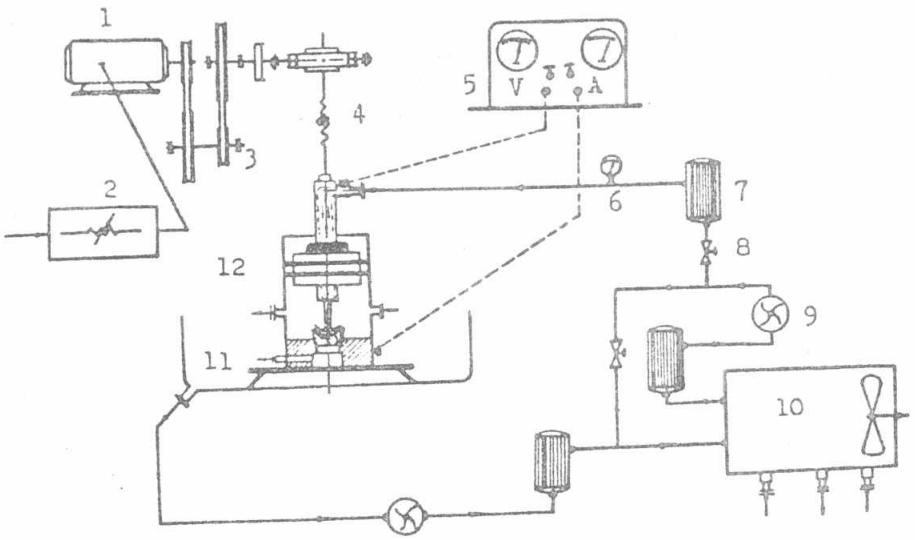

1. Motor
2. Variable resistance
3. Reduction Unit
4. Feed system
5. D.C. power supply
6. Pressure gauge
7. Filter
8. Valve
9. Pump.
10. Tank
11. Insulation
12. Machining cell.

Fig.3: Schematic diagram of EC machine.

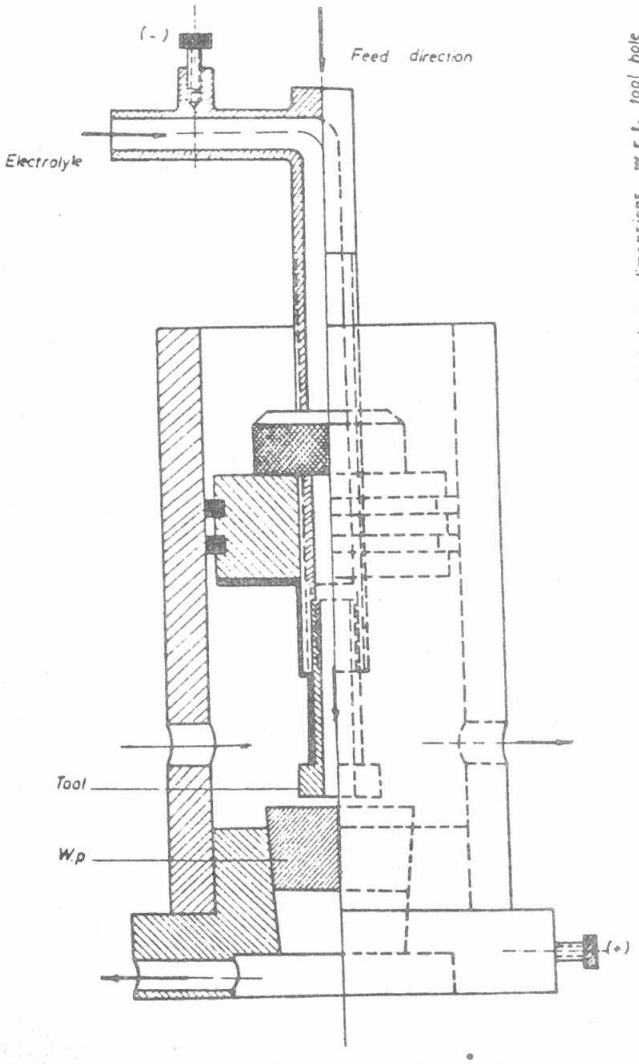

Fig.4. Locally designed machining cell.

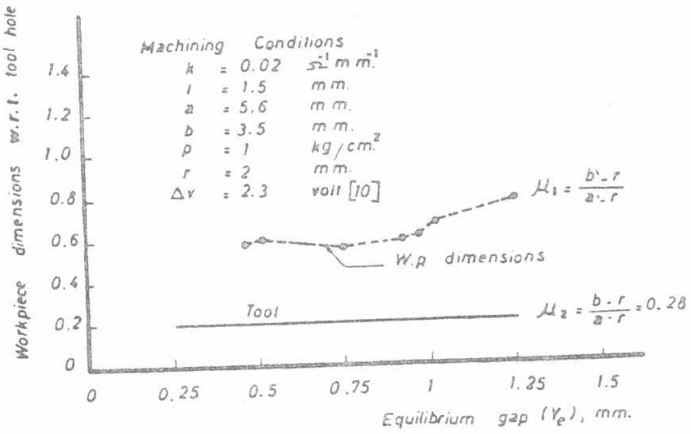

Fig.5 Effect of equilibrium gap on workpiece dimensions

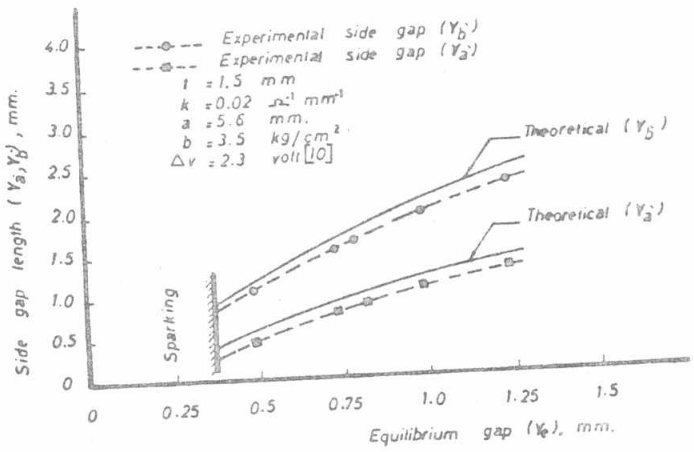

Fig. 6 Effect of equilibrium gap on side gap length

The difference between the two side gaps has been attributed to the inequality of the current flow line at area ($A_{\bar{a}}$ and area ($A_{\bar{b}}$) as illustrated in Fig. 7. Gap correcting factor (ν) was found to be 1.2, as the present experimental tests have revealed, and as was discussed before by Kawafune et al. [6] . Side gap at the major diameter ($Y_{\bar{a}}$) was found to be a function in the side gap at the minor diameter ($Y_{\bar{b}}$). The correlation between them has been extracted from figures 4 and 5 and is expressed as follows :

$$Y_{\bar{a}} = (0.48 : 0.56)\, Y_{\bar{b}}$$

However, it has been found that the increase in the frontal current density was more than ($A_{\bar{b}}$) because of the increase in the tool area exposed to the electrolysing current.

Distribution of current density at the workpiece surface (Fig. 7), is more regular at area ($A_{\bar{a}}$) than at area ($A_{\bar{b}}$). This variation defines the feature of the curvature of the workpiece profile at these areas. For equilibrium gaps less than 0.35 mm, sparking tends to occur at the tool side in the direction of the major diameter [7] and cause tool damage. The conditions of cavitation and dead water zone [8] are also likely to arise at this region which suffers from a sudden decrease in the local pressure of flow (Fig. 8) Furthermore, hydrogen, which is produced by ECM action at this area, forms large bubbles in the electrolyte stream, and consequently resists the passage of the electrolysing current at that region [9] .

Figure 9 shows that as the applied voltage increases, the consumed current increases. This can be explained by the increase in the equilibrium gap value at the high applied voltages.

Figure 10 shows that the feed rate is the most vital factor affecting the consumed current. The maximum feed rate reached was 2 mm/min. The lack of using higher feed rates was attributed to the decrease in the side gap length at the major diameter (0.3 mm) which is considered the favourable zone to generate the severe sparking and causes the tool damage. Furthermore, at rising tool feed rates, a proportionate increase in flow will be required with corresponding increase in pressure which has not been realized during this investigation.

Figure 11 shows that as tool land increases, the consumed current increases. The tool land has been selected on practical considerations to resist tool deformity and tool vibrations. Tool land has also been restricted to 2.5 mm in order to minimize side current, workpiece conicity and stray machining.

Figure 12 shows the values of current density values which have been achieved during this work.

CONCLUSION

- Elliptical holes by ECM have a complexity nature due to the irregularity of electrolyte distribution and different current density along the workpiece surface.
- Modified resistance model technique proved to be adequate to predict

the geometry of workpiece profile and power consumption for the elliptical holes by ECM.

- Feed rates have been restricted to 2 mm/min. because of the generation of the severe sparking at tool surface in the direction of the minor diameter.

- Future researches can be devoted to the utilization of reverse flow or restricted flow, to verify more electrolyte distribution on workpiece surface and to get higher feed rates.

REFERENCES

1- Ebeid, S.J., "Side Gap Estimation in Electrochemical Drilling", Int. MDP - Conf. 1, TECH - 17, Egypt, (1979).
2- Jain, V.K., and Pandey, P.C., " Application of Finite Element Technique to Electrochemical Machining". J. Eng. Prod., Vol. 3, 135 - 148, India,(1980).
3- Hewidy, M.S., and Mahmoud, A.A., "Some Problems Associated with Shape Prediction in ECM", presented at AIMTDR - Conf. 11, Madras, (1984).
4- Ghabrial, S.R., Nasser, A.A., Ebeid, S.J., and Hewidy, M.S., "Electrochemical Wire Cutting". Int. MTDR Conf. 24, 323 - 328, (1983).
5- Vygodsky, M., "Mathematical Handbook - Higher Mathematics", Mir Publishers, Moscow, (1978).
6- Kawafune, K., Mitkoshiba, T., and Otto , K., "Study on Shapes Processed by ECM", Ann. of CIRP, Vol. 16, 345 - 352, (1968).
7- Ebeid, S.J., Baxter, E.M., and Larsson, C.N., "Further Effects of Process Parameters on the Incidence of Sparking in ECM",(1978).
8- Dietz, H., Gunlher, K.G., and Otto, K., "ECM Calculation of Side Gap with Respect to Hydrogen Evolution"., Ann. of CIRP, Vol. 23/1, 45 - 64, (1974).
9- McGeough, J.K., "Principles of ECM", Chapman and Hall, London, (1974).
10- König, W.K., and Humb, H.J., "Mathematical Model for the Calculation of the Contour of the Anode in ECM"., Ann. of CIRP, Vol. 22/1, 83 - 87, (1977).

NOMENCLATURE

A	Cross(sectional area of the electric resistance.
A_a-, A_b-, A_{ab}-	See Figure 2.
A_f-	Frontal area of the workpiece profile.
a	Major radius of the elliptical tocl.
$\bar{a}$	Major radius of the resultant workpiece profile.
b	Minor radius of the elliptical tool.
$\bar{b}$	Minor radius of the resultant workpiece profile.
e	Eccentricity of the ellipse.
F	Faraday's constant.
f	Feed rate.
$\bar{f}$	Frontal direction.
J	Current density.
K	Electrolyte electrical conductivity.
L	Length of the elliptic arc.
r	radius of the hole of electrolyte supply.
R	Electric resistance.

6

$R_{\bar{a}}, R_{\bar{b}}, R_{\bar{a}\bar{b}}, R_{\bar{f}}$	Electric resistance at the area $A_{\bar{a}}$, $A_{\bar{b}}$, $A_{\bar{a}\bar{b}}$, $A_{\bar{f}}$
t	Length of tool land.
v	Applied voltage.
Y	Interelectrode gap.
$Y_{\bar{a}}, Y_{\bar{b}}, Y_{\bar{a}\bar{b}}, Y_e$	See Figure 2.
P	Electrolyte pressure.
ϵ	Chemical equivalent.
η	See Fig. 2.
κ	Gap correcting factor between $Y_{\bar{a}}$ and $Y_{\bar{b}}$.
κ_2	See Fig. 5
κ_1	Gap correcting factor between $Y_{\bar{b}}$ and Y_e .
ρ_ω	Density of workpiece material.

Machining conditions

Y_e = 0.38 mm,
I = 150 Amp.
J = 100 Amp/mm^2
2a = 11.2 mm
2b = 7 mm
Y_a = 0,7 mm
Y_b = 0.4 mm.

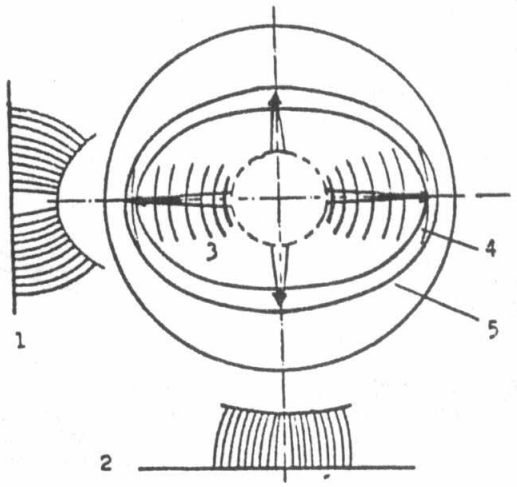

1. Distribution of current flow lines at area $A_{\bar{a}}$
2. Distribution of current flow lines at area $A_{\bar{b}}$
3. Pressure distribution 4. Tool
5. Workpiece profile.

Fig. 7: Pressure and current flow lines distribution.

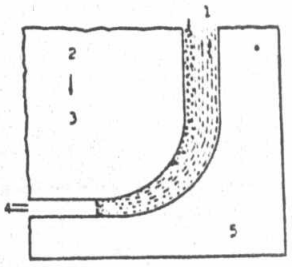

1. Dead zone with gas bubble formation 2. Tool
3. Direction of feed 4. Electrolyte
5. Workpiece

Fig. 8 Schematic diagram illustrating formation of dead water zone by flow breakaway.
after Dietz et al.[8]

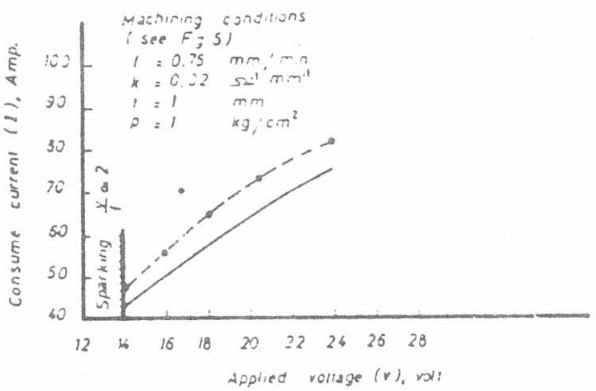

Fig. 9 Effect of applied voltage on consumed current.

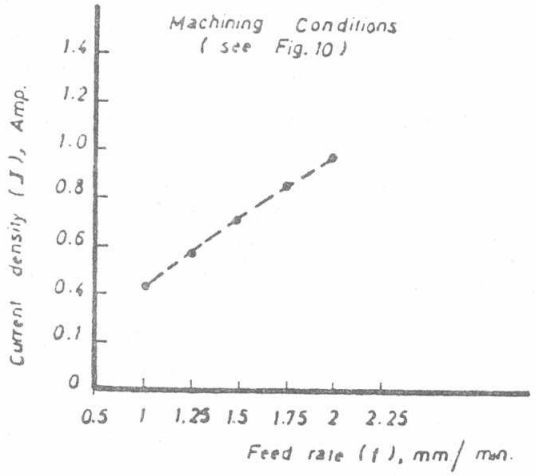

Fig. 12 Effect of feed rate on current density.

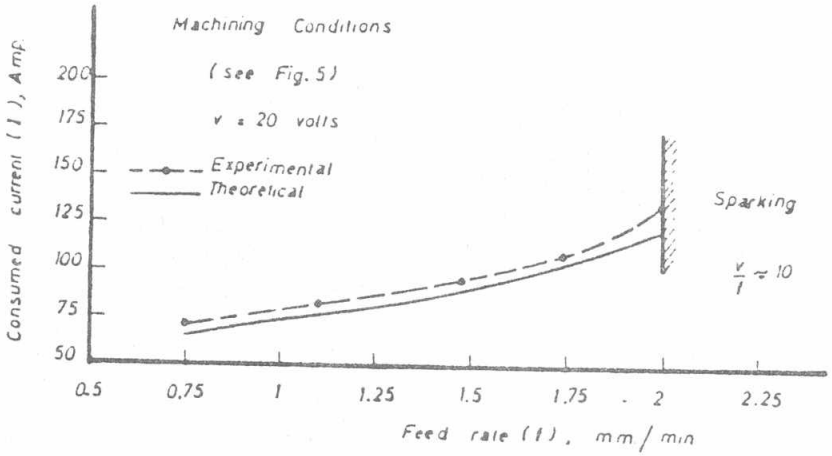

Fig. 10 Effect of feed rate on consumed current.

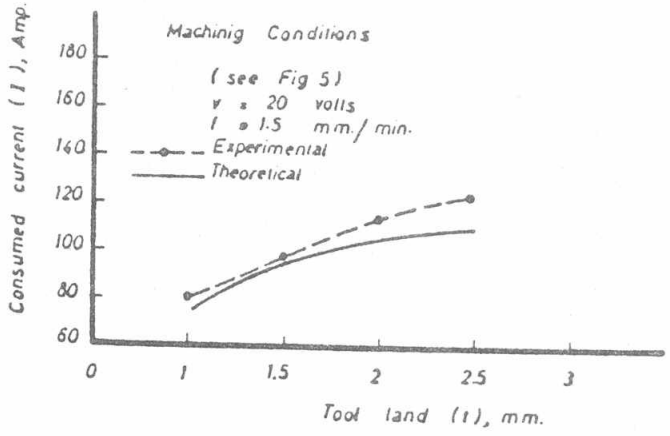

Fig. 11 Effect of tool land on the consumed current.